大阪公立大学
Osaka Metropolitan University
学術情報リポジトリ

Semiempirical Models for Depth-Dose Curves of Electrons in Matter : An Introductory Review

メタデータ	言語: eng 出版者: 公開日: 2010-04-06 キーワード (Ja): キーワード (En): 作成者: Tabata, Tatsuo メールアドレス: 所属:
URL	https://doi.org/10.24729/00008385

Bulletin of University of Osaka Prefecture
Vol. 41, No. 2, 1993, pp.103–118.

Semiempirical Models for Depth–Dose Curves of Electrons in Matter: An Introductory Review*

Tatsuo TABATA**

(Received October 30, 1992)

The basic principle of a semiempirical model, proposed by Kobetich and Katz, for depth–dose curves of electrons in homogeneous semi-infinite absorbers is described. The development, by the present author and his coworker, of an algorithm based on this model is reviewed. A possible method of further improvement of the algorithm is briefly described, and examples of new Monte Carlo data to aid the improvement are shown. An outline and some examples of application are also described of a semiempirical model for multilayer absorbers.

1. Introduction

Because of short path-lengths of electrons in matter, electron beams used for radiation processing give doses that change rapidly as a function of depth. This situation sharply contrasts with almost uniform absorbed-dose distributions given by Co-60 gamma-rays, which is another type of radiation commonly used for radiation processing. In using electron beams, therefore, it is important to have accurate knowledge of the depth–dose profile as a function of electron energy and absorber atomic-number.

There are three important elementary processes electrons experience in their passage through matter: (1) energy loss by collision with atomic electrons, (2) energy loss by radiative process (bremsstrahlung emission) in the Coulomb field of atomic nuclei and (3) elastic scattering by the Coulomb field of atoms (the cumulative effect of this is called multiple scattering). Each elementary process and the cumulative effect of each can be described by analytic formulas. However, these formulas neglect influences of the other elementary processes, and are applicable only to absorbers of thicknesses small compared with the range of incident electrons in matter.

For larger thicknesses we cannnot neglect mutual influences of the different processes, so that the problem of the passage of electrons through thick layers

---

* Translated and adapted from: T. Tabata, Hoshasen-Kagaku (Radiation Chemistry) No. 53, 2 (1992) (in Japanese) .

** Research Institute for Advanced Science and Technology.

of matter is difficult to treat analytically. To overcome this difficulty, other theoretical approaches of the Monte Carlo method and numerical solving of the transport equation have been used. Recently a third method of simplified analytic-modeling began to be used for application purposes. Garth[1] was the first to classify theoretical approaches to electron-transport problems into the above three categories. In the next paragraphs, a simple explanation of these three categories of method is given partly referring to his description.

The Monte Carlo method is an experiment with a computer, so to speak. We can simulate every physical process rather faithfully by this method, but it takes a long computation time with big computers to obtain results with small statistical uncertainties.

The method of numerical solving of the transport equation gives smooth results less costly than the Monte Carlo method. However, it is difficult with this method to include the effect of energy-loss straggling, and there are also problems of errors due to discretization and of convergence of iterative computation, which make the development of reliable algorithms difficult[1].

The simplified analytic-modeling to describe the interaction of electrons with matter can be classified into two types: one is the semiempirical modeling that uses adjustable parameters, and the other is the simplified theoretical modeling that does not use such parameters. The latter is useful for analyzing the relative importance of competing processes. For most problems, however, it does not reproduce experimental or Monte Carlo data with high accuracy, and is not useful from the point of view of using numerical results.

The method of semiempirical modeling is used to formulate analytic expressions that reproduce the experimental or Monte Carlo data on specific quantities. This method cannot therefore be the means of research to explain the behavior of electrons from the first principles. However, when we have finished the stage of such basic reserach and treat applied problems arising in the use and measurement of electrons or other ionizing radiations (problems related to the latter are often related to those of electrons, by way of the emission of secondary electrons), the method of semiempirical modeling becomes useful.

Advantages of this method are as follows: (1) Solutions can be obtained with pocket calculators or personal computers. (2) A rapid insight into the behavior of specific quantities when absorber atomic-number or incident energy is changed can be gained. (3) When incorporated into a computer program to provide input data for solving more complicated problems, it saves memory space and computation time.

On the other hand, the method of semiempirical modeling has a disadvantage of being inadequate for solving most problems with complex geometry. The present author, however, has been applying this method to a rather complicated problems of evaluating depth–dose curves of electrons in multilayer slab-absorbers as well as formulating analytic equations for specific quantities. In this review, description is made of (1) the basic principle of a semiempirical model for depth–dose curves of electrons in homogeneous semi-infinite absorbers, (2) a

set of new Monte Carlo data on the above depth--dose curves obtained by the present author's group to aid the improvement of the modeling, and (3) the outline and some examples of application of a semiempirical model for depth–dose curves of electrons in multilayer absorber developed by the present author and his coworker.

2. Homogeneous Semi-Infinite Absorbers

2.1 Definitions and reciprocity rule

In speaking about depth–dose curves, it is necessary to define geometrical configurations of electron beams and absorbers. In the present review, we assume that electrons come along parallel lines, from a plane source with an effectively infinite area (a plane-parallel beam or broad beam). We assume also that the electrons are normally incident on a slab absorber with an effectively infinite area. In this section, consideration is restricted to homogeneous absorbers of effectively semi-infinite thickness. The situation in which plane-parallel beams are normally incident on semi-infinite absorbers is most important as the basis of different configurations.

In comparing absorbed doses for different incident-energies and absorber atomic-numbers, it is necessary to use doses for a definite number of incident electrons. Therefore, we use the quantity, "absorbed dose per unit fluence." Here fluence is defined as the ratio dN/da when N particles are incident on the sphere of cross-sectional area da.

Lets consider the following two absorbed energies:

(1) The energy absorbed per unit fluence per unit mass at the depth z, i.e., the absorbed dose $D_e(z)$ per unit fluence, when a plane-parallel electron-beam is normally incident on a homogeneous semi-infinite absorber.

(2) The energy absorbed per unit fluence per unit mass-thickness at the depth z over the whole area, when an electron beam coming in a single direction from a point source (a pencil beam or narrow beam) is normally incident on the same homogeneous semi-infinite absorber as assumed in (1).

These two energies are equal to each other, and this relation is called the reciprocity rule. Because of this rule, the depth-dose curves for the following two geometrical configurations are almost the same:

(1) A large-area sample is irradiated by a curtain-shaped electron beam or a scanned electron-beam with a small scanning-angle, and the depth–dose curve is measured with a small detector along the center-line of the beam.

(2) A large-area sample is irradiated by a narrow-beam, and the depth–dose curve is measured with a thin large-area ionization chamber inserted perpendicularly to the beam.

2.2 The basic principle of a semi-empirical model

Kobetich and Katz[2,3] made an algorithm for the depth–dose curve of electrons on the basis of the fact that the absorved dose $D_e(z)$ described above can approximately be expressed by

$$D_e(z)dz = \{-d[\eta(z)E(z)]/dz\}\, dz. \tag{1}$$

Here $\eta(z)$ is the number-transmission coefficient of electrons normally incident on a slab absorber, and $E(z)$ is the residual energy of the electrons transmitted through this absorber. If we neglect the backscattering of electrons both at the incident surface and inside the absorber, the quantity $\eta(z)E(z)$ is equal to the energy, per incident electron, transmitted through the depth z in the semi-infinite absorber, and Eq.(1) expresses the simple fact that the energy given to the absorber is equal to the amount of reduction in the average energy possessed by the incident electrons.

In spite of its simplicity, the usefulness of Eq.(1) is large. If we know two functions $\eta(z)$ and $E(z)$ as a function not only of z but also of incident-electron energy and absorber atomic-number, we obtain a general expression for $D_e(z)$. Empirical equations for $\eta(z)$ has been studied by a number of authors (for example, see Ref. 4). A good approximation to $E(z)$ can be obtained by an inverse of the function to express the extrapolated range as a function of electron energy.

Performing the differentiation on the right-hand side of Eq.(1), we obtain

$$D_e(z)dz=(-d\eta/dz)Edz+\eta(-dE/dz)dz. \tag{2}$$

If we neglect the effect of backscattering again, the factor $(-d\eta/dz)$ in the first term of the right-hand side of Eq.(2) is equal to the projected-range distribution of the incident electrons in the semi-infinite absorber. It increases with increasing z and reaches a maximum at the most-probable projected range. On the other hand, both the functions $E(z)$ and $\eta(z)$ decrease with increasing z, and $(-dE/dz)$ is almost constant for a wide region of z from 0 to a large fraction of the extrapolated range. The depth–dose data show that $D_e(z)$ initially increases with increasing depth (this portion of the depth–dose curve is called the buildup region), reaches a maximum, and then decreases (see Fig. 1). From these trends of $D_e(z)$ and of factors on the right-hand side of Eq.(2), we see that the initial rise of $D_e(z)$ comes from $(-d\eta/dz)$.

However, we have to be careful not to give a rigorous physical interpretation to the right-hand side of Eq. (2), because such an interpretation lead to a paradoxical conclusion. We might interpret that the first term represents the energy deposition by the electrons that come to a stop at the depths between z and $z+dz$, and that the second term represents the energy deposition by the electrons that pass through the same interval of depth. When we combine this interpretation with the numerical value of the function $E(z)$, we arrive at the conclusion

that the energy of the electrons that are stopped within a same size of depth interval dz is much different, depending on depth. This contradicts the actual situation.

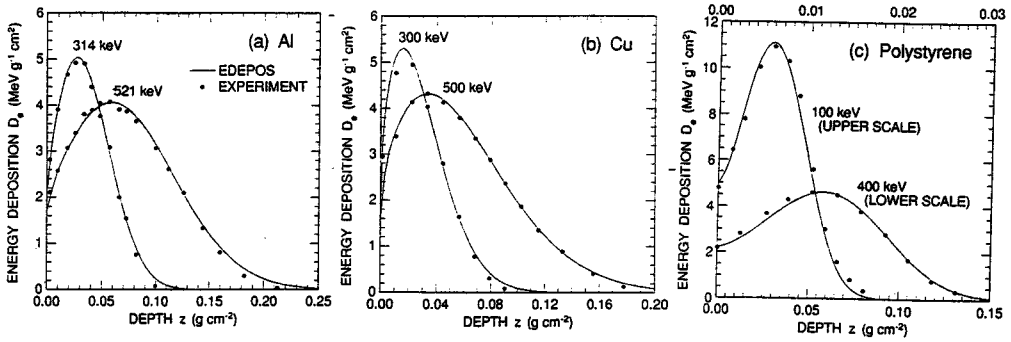

Fig. 1 Depth–dose curves of electrons in (a) Al, (b) Cu and (c) polystyrene. Curves, the EDMULT code; points in (a) and (b), experimental data by Lockwood *et al.*[9]; points in (c) experimental data by McLaughlin *et al.*[8]

The reason for the above contradiction lies in the fact that in expressing the transmitted energy by a simple product of two terms we have neglected the energy and angular distributions of transmitted electrons. Therefore, we should not apply physical interpretation to each term of the right-hand side of Eq. (2), even though the product $\eta(z)E(z)$ and the right-hand side of Eq. (2) are good approximations of the transmitted energy and the energy deposition. It is to be noted that factors not considered in Eq. (2) play an important role for the buildup of the depth–dose curve. Such factors are (1) the gradual deviation of the paths of electrons from the initial direction due to multiple scattering and (2) the contribution of secondary knock-on electrons produced by the incident electrons and bremsstrahlung photons. The neglect of these sets a limitation to the semiempirical model.

2.3 The EDEPOS code

We have incorporated the following corrections into the algorithm of Kobetich and Katz to obtain higher accuracy[6]: (1) a correction for the energy carried away by electrons backscattered from the surface of the medium and (2) a correction for the energy carried away by bremsstrahlung photons to the depths greater than the maximum range of the incident electrons. These corrections appear in a multiplication factor applied to the right-hand side of Eq. (1). Thus we have the following equation instead of Eq. (1) :

$$D_e(z)dz=(1-f_b-f_r)\{-d[\eta(z)E(z)]/dz\}dz, \tag{3}$$

where f_b is the fraction of the incident energy backscattered from the incident

surface and f_r is the fraction of the incident energy deposited at the depths corresponding to the bremsstrahlung tail of the depth–dose curve. The FORTRAN code to perform our algorithm is called EDEPOS, and is applicable to incident energies from about 0.1- to 20-MeV and absorber atomic-numbers from 5.28 (an effective atomic-number for polystyrene) to 82.

Originally the function $E(z)$ was made by using an empirical equation to express the energy of electrons as a function of their extrapolated range in matter; and the equation was replaced by an exponentially decaying function at a large depth, to prevent $E(z)$ from suddenly dropping to zero. However, such an expression produces a spurious deflection of the curve at a large depth, through the term of dE/dz. We made a revision of the EDEPOS code to remove this defect and to obtain better accuracy[6,7]. Lines in Fig. 1 represent depth-dose curves given by the improved EDEPOS code, and show its good reproducibility of experimental data[8,9].

2.4 Reference data and a possible method of further improvement

A rather small number of reliable data-sets have been available on the depth–dose curve of electrons normally incident on semi-infinite absorbers. When we first developed the EDEPOS code, we used 29 sets of experimental data, collected from literature, for absorber atomic-numbers from 5.28 to 82 and incident energies from 0.3 to 20 MeV as well as seven supplementary sets of Monte Carlo data generated by the ETRAN code[10]. The incident energies for most of the data sets were in the energy region around 1 to 2 MeV. The data for the absorber atomic-numbers above 29 and for energies above 5 MeV were extremely scarce. Later Lockwood *et al.*[9] published experimental and Monte Carlo data for energies between 0.05 and 1 MeV, but the situation of data deficiency did not change much.

In 1986 Rogers *et al.*[11,12] compared the depth–dose curves of electrons in water generated with the EGS4 Monte Carlo code[13] and with ETRAN. They pointed out the possibility that the latter code, which had been considered to be an almost complete Monte Carlo code for the penetration of electrons and photons, had a defect. This led to the improvement of the method used in ETRAN for sampling the energy-loss straggling[14], and agreement of the results obtained with the two codes improved[15]. Thus the reliability of the present version of the ETRAN code and the Integrated TIGER Series (ITS) code-system[16] based on it has been increased further.

We started a plan to generate with ITS a systematic set of depth–dose data for incident energies from 0.1 to 100 MeV and for absorber atomic-numbers from 4 to 92 and to improve the EDEPOS code by analyzing these data. The Monte Carlo calculation was already finished and the results have been published[17]. Figure 2 shows examples of the depth–dose curves obtained. In Fig. 2b, the axes are scaled by using the continuous slowing-down approximation range r_0 and the incident energy T_0. It is to be noted that in this scaling the depth–dose curves are almost the same for energies from 0.1 to 1 MeV. This is one of the

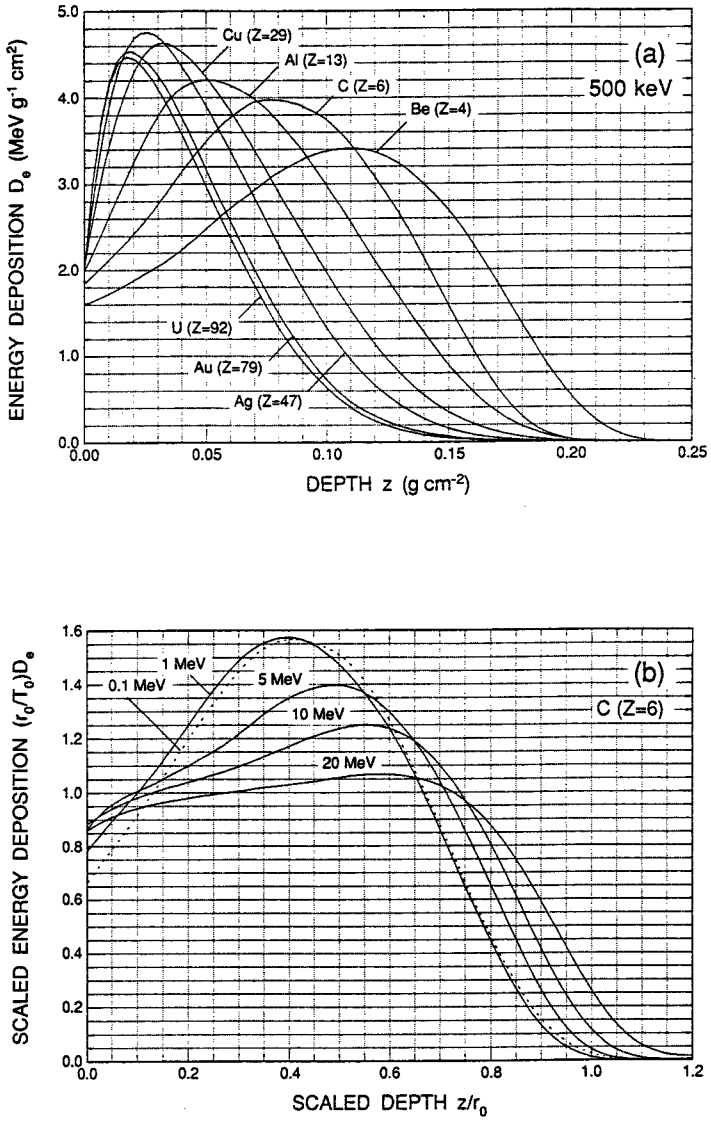

Fig. 2 Examples of depth–dose curves obtained with the ITS Monte Carlo code system. (a) 500-keV electrons incident on different absorbers, (b) 0.1- to 20-MeV electrons incident on C. Data have been taken from Ref. 17; numerical smoothing has been applied.

manifestations of the scaling rule of electron penetration discussed by Harder[18].

For medical treatment with electron beams, accurate knowledge on the depth–dose curves in water, as the material equivalent to tissue, is necessary. To respond to this necessity, we formulated[19] a depth–dose algorithm that is applica-

ble only to water but has much higher accuracy than EDEPOS (Fig. 3). In this algorithm, the component of the energy deposition through radiative process is expressed by a separate function, and the values of adjustable parameters in the expression were optimized to reproduce the results of three Monte Carlo codes, MCEF[20], ITS and EGS4. We are planning to apply a similar method to the improvement of EDEPOS.

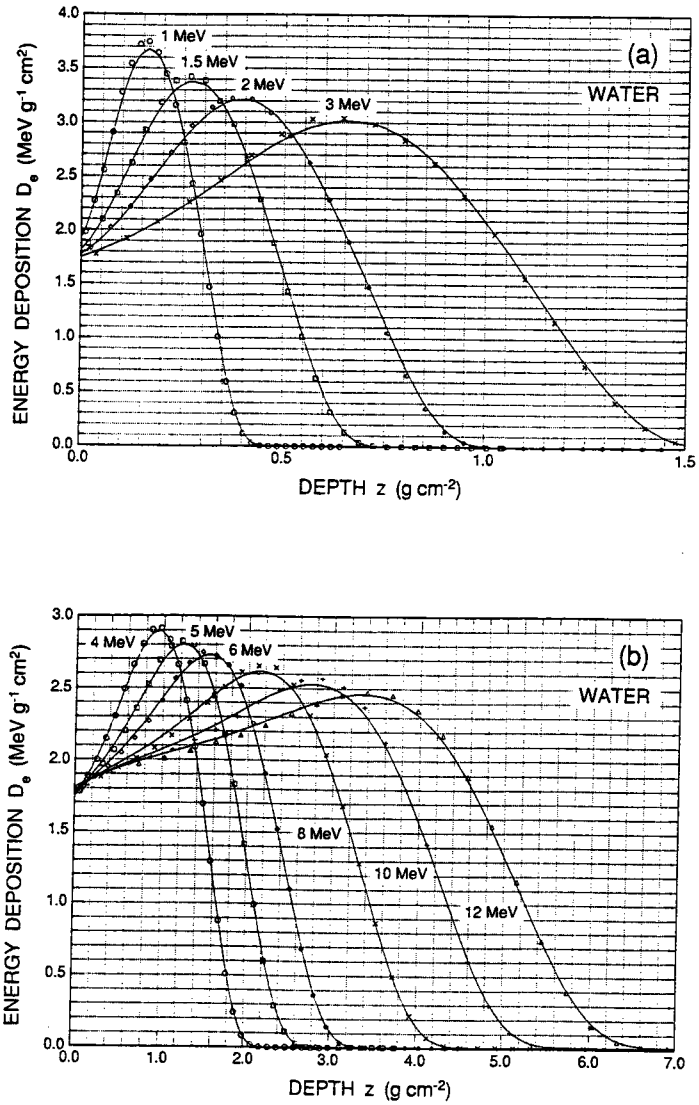

Fig. 3 Depth–dose curves of electrons in water. Curves, the analytic expression of Tabata *et al.*[19]; points, Monte Carlo results with the MCEF code reported by Andreo[15]. (a) 1–3 MeV, (b) 4–12 MeV.

3. Multilayer Absorbers

3.1 Necessity of semiempirical models and the EDMULT code

In using electron beams for radiation processing, electrons from accelerators pass through the accelerator window and intervening air-layer, and suffer energy loss and scattering before impinging on samples to be irradiated. The samples are often attached to the backing material made of metal, which produces considerable effect of backscattering. To evaluate the absorbed dose in the sample, therefore, it is necessary to solve the problem of electron transport through a multilayer consisting of three or four component layers.

At first sight it might seem that the Monte Carlo method or the transort-equation method is indispensable to solve such a complex problem of evaluating depth–dose curves of electrons in multilayer absorbers (as for the treatment with these methods, see Refs. 9, 21–25). However, the present author and his coworker considered that a semiempirical model for this problem can be constructed by the repeated use of depth–dose curves for homogeneous semi-infinite absorbers described in the previous section, and tried formulation of an algorithm based on such a model[26].

The FORTRAN code we developed to execute this algorithm is named EDMULT (an acronym of *e*nergy *d*eposition in *mult*ilayer absorbers)[27, 28]. The code is applicable to the same regions of incident energies and absorber atomic-numbers as those for the EDEPOS code. The numbers of layers that can be treated were originally up to three, but are now being extended up to four in the cooperative work with Wang. The code package of EDMULT including related documents is available from Radiation Shielding Information Center, Oak Ridge National Laboratory, by sending a floppy disk for transmittal of the code.

3.2 The algorithm of EDMULT

The outline of the algorithm used in the EDMULT code is explained here with an example of the simplest multilayer, i.e., the two-layer absorber. As shown in Fig. 4, we call the region devoid of material "region 0," and the next two regions filled with materials m_1 and m_2 "region 1" and "region 2," respectively. In region 1, s_{10} represents the path segment of the electrons that pass region 1 after impinging there directly; and s_{12}, the path segment of the electrons that run backward after being backscattered in region 2. In region 2, s_{20} represents the path segment of the electrons that pass through region 2 just after passing through region 1; and s_{21}, the path segment of electrons that pass through region 2 after being backscattered twice, i.e., once in region 2 and then in region 1.

If we neglect the effect of the third and more times of backscattering, it is sufficient to evaluate the dose components from the above schematic path-segments by using the algorithm for semi-infinite absorbers. It is to be noted here that the contributions from the branched path-segments have to be multiplied by a weight proportional to the energy-backscattering coefficient. The applicabiliy of the above modeling owes to the fact that the effect of the presence of differ-

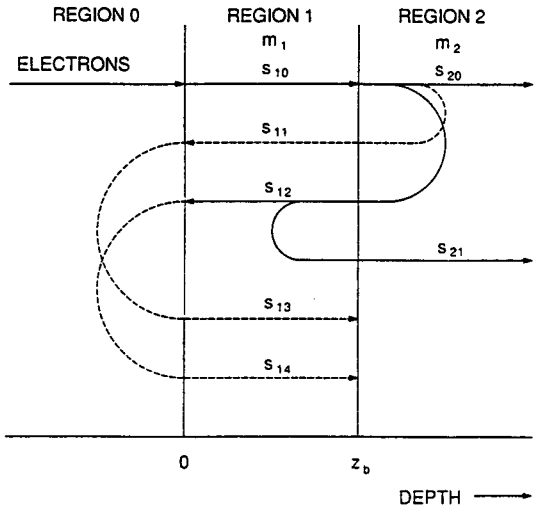

Fig. 4 Schematic diagram showing electron paths assumed in the semiempirical model to evaluate depth–dose curves in two-layer absorbers[26]. Dashed lines show virtual paths necessary for correction.

ent layers arises mostly from the difference in backscattering of electrons across the interface.

In constructing details of the multilayer depth–dose algorithm, we should take into consideration special corrections arising from the use of the algorithm for semi-infinite absorbers. For example, the result, given by the latter algorithm, for the contribution to the dose from the path segment s_{10} includes the effect of backscattering by material m_1 in region 2 (the path segment related to this effect is shown by s_{11} in Fig. 4). This effect, however, is not present in the multilayer absorber, so that we have to remove it. In addition to s_{11}, we must consider similar corrections related to virtual path-segments shown by s_{13} and s_{14} in Fig. 4.

Among different contributions, those from path segments s_{12}, s_{20} and s_{21} require special treatment, because the material through which electrons have just been transmitted is different from the material in which they are now passing. As an example, let us consider the contribution from s_{20}. The electrons reaching the interface between regions 1 and 2 have passed through the layer thickness z_b consisting of material m_1. If we replace this layer by an equivalent layer of thickness z_b' consisting of material m_2, we can use the depth-dose algorithm for the semi-infinite absorber.

We assume here that the equivalence rule proposed by Tanaka *et al.*[19] is applicable. The rule states: In a first approximation, the depth–dose profile in region 2 does not change under such replacement as described above provided that T_r and θ_h of electrons at the interface are unchanged by the replacement (equivalence condition), where T_r represents the residual energy and θ_h is the half-value angle of multiple scattering. To satisfy the equivalence condition, we can adjust

two parameters, i.e., the equivalent thickness z_b and the equivalent incident energy.

To calculate the dose contribution by electrons backscattered through the interface between two media, knowledge is necessary of the number- and energy-backscattering coefficients for the electron flux having different angular distributions caused by multiple scattering. Further, the backscattering coefficients have to be evaluated for the absorbers not only of semi-infinite thickness but also of different finite thicknesses.

There are enough data on the number-backscattering coefficient for the basic condition in which electrons are normally incident on semi-infinite absorbers. However, data for other geometrical configurations are scarce. Therefore, by modifying the empirical equation for the basic condition on the basis of certain assumptions, expressions to evaluate backscattering coefficients for different conditions were made, and are used in the EDMULT code. Values of adjustable parameters used in these expresions were optimized so as to minimize the deviation of EDMULT results from experimental and Monte Carlo depth–dose data in literature[9,21,22]. In Figs. 5 and 6, depth–dose curves in two- and three-layer absorbers given by the EDMULT code are compared with the experimental and Monte Carlo results of Eisen *et al.*[22] and Lockwood *et al.*[9]

In the earlier versions of EDMULT, the dose component due to electrons backscattered from the layer of finite thickness was evaluated by taking the difference of dose components due to electrons backscattered from two semi-infinite absorbers displaced by a distance equal to the thickness of the relevant layer.

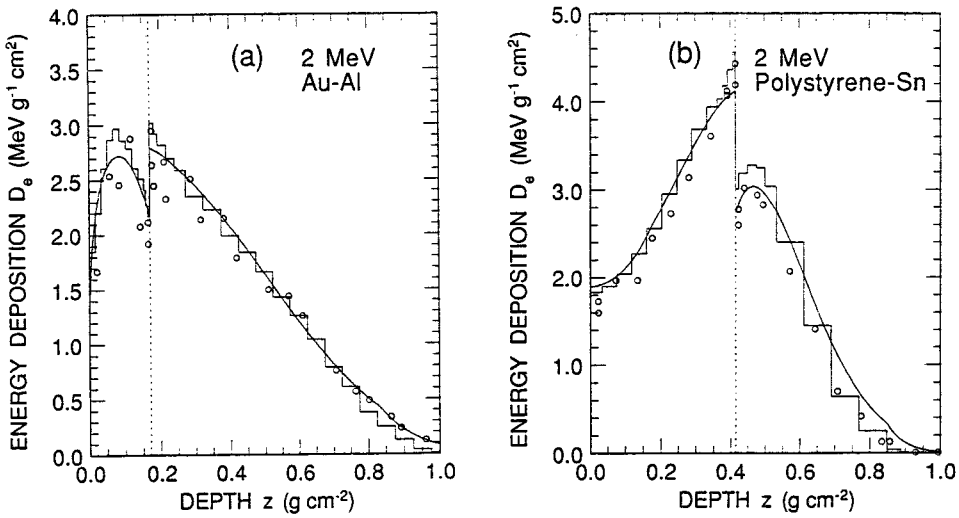

Fig. 5 Depth–dose curves of 2-MeV electrons incident on two-layer slab absorbers consisting of (a) gold and aluminum and (b) polystyrene and tin. Curves, the result of the EDMULT code ; circles and histograms, experiment and Monte Carlo calculation by Eisen *et al.*[22]

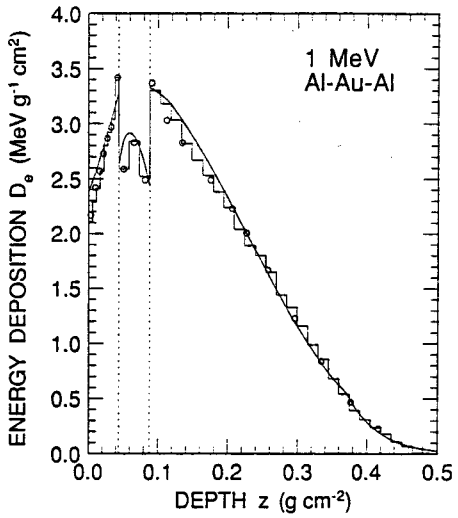

Fig. 6 Depth–dose curves of 1-MeV electrons incident on a three-layer slab absorber consisting of aluminum, gold and aluminum. Curves, the result of the EDMULT code; circles and histograms, experiment and Monte Carlo calculation by Lockwood *et al.*[6]

However, the evaluation mentioned has a possibility of producing large errors for small layer thicknesses. In the latest versions, the evaluation was replaced by the method of using an expression for the backscattering coefficients for the absorbers of finite thicknesses, and minor errors in the earlier versions were corrected[30]. These modifications improved the agreement of EDMULT results with the experimental and Monte Carlo data, especially for dose distributions in the second layer in three-layer absorbers (see Fig. 6).

3.3 Examples of application of EDMULT

Using EDMULT, we can simply evaluate the dependence of absorbed dose in the sample upon the following parameters: (1) the initial energy of electrons or the accelerating voltage, (2) the atomic numbers of the materials that form the sample, the accelerator window and the backing and (3) the thicknesses of the sample, accelerator window and the intervening air layer.

The accelerator window, the air layer, the sample and the backing material make up a system of four layers. To evaluate the absorbed dose in the sample, however, we need not know the dose distributions in the window and the air layer. Therefore, we can treat these two layers as a single layer consisting of a material with an effective atomic-number intermediate between those of the two layers, and apply the code for the three layers[31].

Table 1 shows the effect of backing materials on the absorbed dose in a 50.8-

Table 1 Absorbed dose in a 50.8-μm nylon dosimeter placed on different backing materials[30]. The incident energy of electrons is 400 keV. The geometrical configuration of irradiation is shown on the right of Fig. 7. The column denoted as Seltzer & Berger represents Monte Carlo results with the ZTRAN code[25].

Backing material	Absolute dose (MeV g^{-1} cm^2)		Relative dose	
	EDMULT	Seltzer & Berger	EDMULT	Seltzer & Berger
Nylon	4.07	4.56	1.00	1.00
Al	4.81	5.39	1.18	1.18
Fe	5.72	6.41	1.40	1.41
Cu	5.85	6.61	1.44	1.45
Ag	6.46	7.32	1.59	1.61
Au	7.12	8.15	1.75	1.79
U	7.33	8.50	1.80	1.86

μm nylon-film dosimeter evaluated with EDMULT. The geometrical condition assumed is shown in the right half of Fig. 7. After impinging normally on a titanium window of 25.4-μm thickness, the electron beam with an initial energy of 0.4 MeV passes through an air layer of 10-cm thickness. The Monte Carlo results of Seltzer and Berger are also shown for comparison. The deviations of the EDMULT results from the Monte Carlo results are from 11 to 14% in absolute dose, and from 0 to 3% in relative dose. These values of deviation indicate that the evaluation of the relative effect of different backing materials with EDMULT is highly reliable. The left half of Fig. 7 shows the same result for the relative dose as given in Table 1 together with additional results for differ-

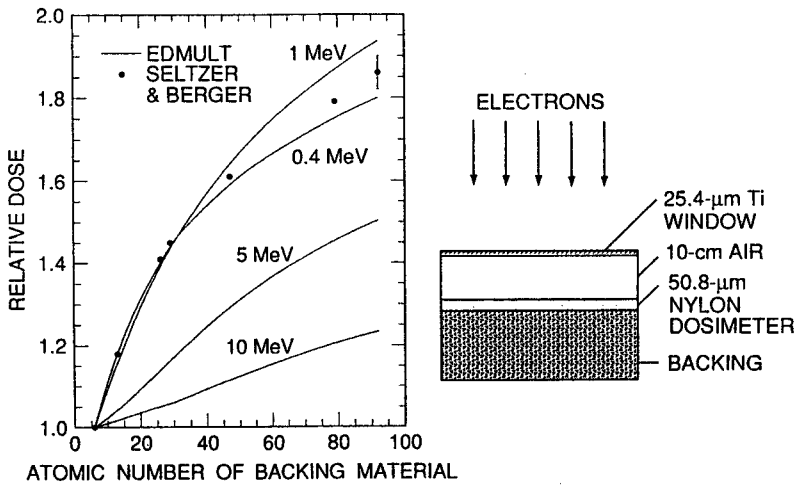

Fig. 7 Relative absorbed dose in a nylon-film dosimeter is plotted as a function of atomic number of the backing material. Curves, the results of the EDMULT code; circles, Monte Carlo calcluation of Seltzer and Berger[25].

ent initial energies of 1, 5 and 10 MeV.

Figure 8 shows another example of application of the EDMULT code. The absorbed dose in the same nylon-film dosimeter as described above is plotted as a function of the thickness of the air layer between the accelerator window and the sample. The geometrical condition assumed is shown in the right half of the figure. For energies above 0.4 MeV, the curves of the figure reflect the initial build-up portion of depth–dose curves of electrons in air; for energies below 0.35 MeV, the curves reflect the portion of similar depth–dose curves up to the maximum and beyond.

Thompson *et al.*[32] reported the results of studies, carried out with EDMULT, on the relation between the absorbed dose and irradiation conditions for electron-beam processing. Among the results, there is an interesting one that shows the degree of uniformity of absorbed dose over the thickness of a sample for different initial energies. They considered a polystyrene sheet irradiated with electrons after passing through a titanium window and an air layer; there was the steel plate of a conveyor behind the sheet. They found that by optimizing the energy it was possible to obtain a fairly uniform dose distribution in a single-sided treatment process with medium-energy equipment of 500 to 600 kV.

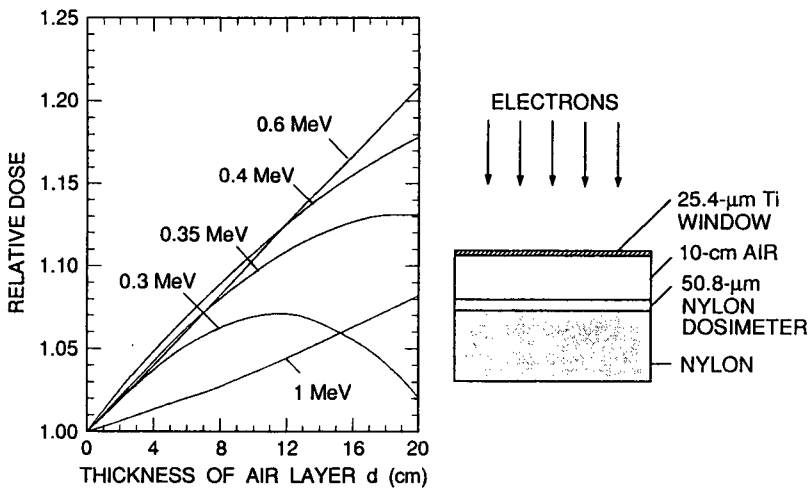

Fig. 8 Relative absorbed dose in a nylon-film dosimeter is plotted as a function of thickness of the air layer that is present between the accelerator window and the dosimeter. Curves, the results of the EDMULT code; circles, Monte Carlo calculation of Seltzer and Berger[25].

4. Concluding Remarks

Matsuda and Kijima[33] measured absorbed doses in single-layer and multilayer absorbers with a CTA dosimeter for 0.3- and 0.8-MeV electrons. Chen *et al.*[34]

studied depth–dose distributions of an electron beam of about 4-MeV energy in multilayer absorbers with PVT and PVT-1 film dosimeters developed by their group. The results of these authors generally agree with the results of EDMULT, within an error of about 10%. On the other hand, the results also indicate the necessity of improving EDMULT for certain conditions.

The algorithm of EDMULT takes into account the effect of energy-loss straggling by the use of empirical depth–dose curves in semi-infinite medium. In evaluating the dose contributions from schematic path-segments arising from backscattering across interfaces, however, we use continuous slowing-down approximation in the sense that the average energy is used by neglecting the spectral distribution. This is a serious limitation of the algorithm. In spite of the limitation, there is a possibility of further improvement of the algorithm by replacing the present sub-algorithm for the single-layer depth–dose curve by an improved one and by making other possible modifications.

Acknowledgments

The author would like to thank Nissin–High Voltage Co., Ltd. and Sumitomo Heavy Industries, Ltd. for financial support to our recent work on semiempirical modeling. He is also indebted to R. Ito for his patient cooperation all through the work of developing the semiempirical models.

References

1) J. C. Garth, Trans. Am. Nucl. Soc., **52**, 377 (1986).
2) E. J. Kobetich and R. Katz, Phys. Rev., **170**, 391 (1968).
3) E. J. Kobetich and R. Katz, Nucl. Instrum. & Methods, **71**, 269 (1969).
4) T. Tabata and R. Ito, Nucl. Instrum. & Methods, **127**, 429 (1975).
5) T. Tabata and R. Ito, Nucl. Sci. & Eng., **53**, 226 (1974).
6) T. Tabata and R. Ito, Proc. Conf. Radiation Curing Asia (CRCA '88), Tokyo, p. 373, Organizing Committee of CRCA, Tokyo (1988).
7) T. Tabata, R. Ito and S. Tsukui, Radiat. Phys. Chem., **35**, 821 (1990).
8) W. McLaughlin and E. Hussman, in "Utilization of Large Radiation Sources and Accelerators in Industrial Processing", p. 579, IAEA, Vienna (1969).
9) G. J. Lockwood, L. E. Ruggles, G. H. Miller and J. A. Halbleib, "Calorimetric Measurement of Electron Energy Deposition in Extended Media — Theory vs Experiment", Report SAND79-0414, Sandia Labs. (1980).
10) RSIC, "ETRAN: Monte Carlo Code System for Electron and Photon Transport", Computer Code Collection CCC-107, Oak Ridge Nat. Lab. (1969).
11) D. W. O. Rogers and A. F. Bielajew, Trans. Am. Nucl. Soc., **52**, 380 (1985).

12) D. W. O. Rogers and A. F. Bielajew, Med. Phys., **13**, 687 (1986).
13) W. R. Nelson, H. Hirayama and D. W. O. Rogers, "The EGS4 Code System", SLAC Report 265, Stanford Linear Accelerator Center (1985).
14) S. M. Seltzer, in "Monte Carlo Transport of Electrons and Photons", T. M. Jenkins, W. R. Nelson and A. Rindi, eds., p. 153, Plenum, New York (1988).
15) P. Andreo, Nucl. Instrum. Methods, **B51**, 107 (1990).
16) J. A. Halbleib, R. P. Kensek, T. A. Mehlhorn, G. Valdez, S. M. Seltzer and M. J. Berger, "ITS Version 3.0: The Integrated TIGER Series of Coupled Electron/Photon Monte Carlo Transport Codes", Report SAND91-1634, Sandia Nat. Labs. (1992).
17) P. Andreo, R. Ito and T. Tabata, "Tables of Charge- and Energy-Deposition Distributions in Elemental Materials Irradiated by Plane-Parallel Electron Beams with Energies between 0.1 and 100 MeV", RIAST-UOP-TR 1, Res. Inst. Adv. Sci. Tech. Univ. Osaka Pref. (1992).
18) D. Harder, Proc. 2nd Symp. Microdosimetry, Stresa, 1969, H. G. Ebert, eds., p. 567, Euratom, Brussels (1970).
19) T. Tabata, P. Andreo and R. Ito, Nucl. Instrum. & Methods, **B58**, 205 (1991).
20) P. Andreo, in "Monte Carlo Transport of Electrons and Photons", T. M. Jenkins, W. R. Nelson and A. Rindi, eds., p. 437, Plenum, New York (1988).
21) M. J. Kniedler and J. Silverman, in "Utilization of Large Radiation Sources and Accelerators in Industrial Processing", p. 567, IAEA, Vienna (1969).
22) H. Eisen, M. Rosenstein and J. Silverman, Radiat. Res., **52**, 429 (1972).
23) I. R. Entinzon, Radiat. Phys. Chem., **27**, 469 (1986).
24) I. R. Entinzon, A. S. Kutsenko and A. A. Chujko, Radiat. Phys. Chem., **37**, 295 (1991).
25) S. M. Seltzer and M. J. Berger, Appl. Radiat. Isot., **38**, 349 (1987).
26) T. Tabata and R. Ito, Jpn. J. Appl. Phys., **20**, 249 (1981).
27) R. Ito and T. Tabata, "Semiempirical code EDMULT for depth–dose distributions of electrons in multilayer slab absorbers: Revision and applications", RCOP-TR 8, Radiation Center of Osaka Prefecture (1987).
28) RSIC, "EDMULT 3.11 MICRO: Electron Depth–Dose Distributions in Multilayer Slab Absorbers", Report CCC-430, Oak Ridge Natl. Lab. (1992).
29) R. Tanaka, K. Yotsumoto and Y. Nakamura, in "Preprints of the 32nd Autumn Meeting Jpn. Soc. Appl. Phys.", p. 231 (1971).
30) T. Tabata and R. Ito, Proc. RadTech Asia '91, Osaka, p. 528, RadTech Jpn., Tokyo (1991).
31) T. Tabata, R. Ito, I. Kuriyama and Y. Moriuchi, Radiat. Phys. Chem., **33**, 411 (1989).
32) C. C. Thompson, H. F. Melone, R. G. Burgess, T. F. Lisanti, M. Masiello and M. R. Cleland, RadTech '90–North Amer. Conf. Proc., Vol. 1, 1990, Chicago, p. 53, RadTech Inst. North Amer., Northbrook (1990).
33) K. Matsuda and T. Kijima, Appl. Radiat. Isot., **42**, 235 (1991).
34) Chen Wenxiu, Chen Lemei, Meng Zhaoxing and S. Navaratnam, Proc. 5th China–Japan Bilateral Symp. on Radiat. Chem., Beijing, 1991 (1992) p. 250.